Supporting materials

Ten-year trend of $PM_{2.5}$ major components and source tracers from 2008 to 2017 in an urban site of Hong Kong, China

Wing Sze Chow[a], Kezheng Liao[a], X. H. Hilda Huang[b], Ka Fung Leung[b], Alexis K. H. Lau[b], Jian Zhen Yu[a,b]
[a]Department of Chemistry, [b]Division of Environment & Sustainability, The Hong Kong University of Science and Technology, Clear Water Bay, Kowloon, Hong Kong, China

This document contains

S1. Site information - Meteorological conditions and traffic flow statistics in Tsuen Wan

The daily meteorological conditions from 2008 to 2017 in Tsuen Wan are summarized in Figure S1. From 2008 to 2017, all the meteorological factors were similar between years. In the summer, both the temperature (27.0 ± 1.5ºC) and the relative humidity (86.6 ± 7.2%) were higher. The precipitation was also higher in summer (107.9 ± 226.0 mm) than that in spring (47.2 ± 127.4 mm), fall (34.5 ± 130.2 mm), and winter (11.2 ± 53.0 mm). The 10-years traffic flow statistics in the Shing Mun Tunnel, which is ~5 km from the Tsuen Wan sampling site, are summarized in Figure S2.

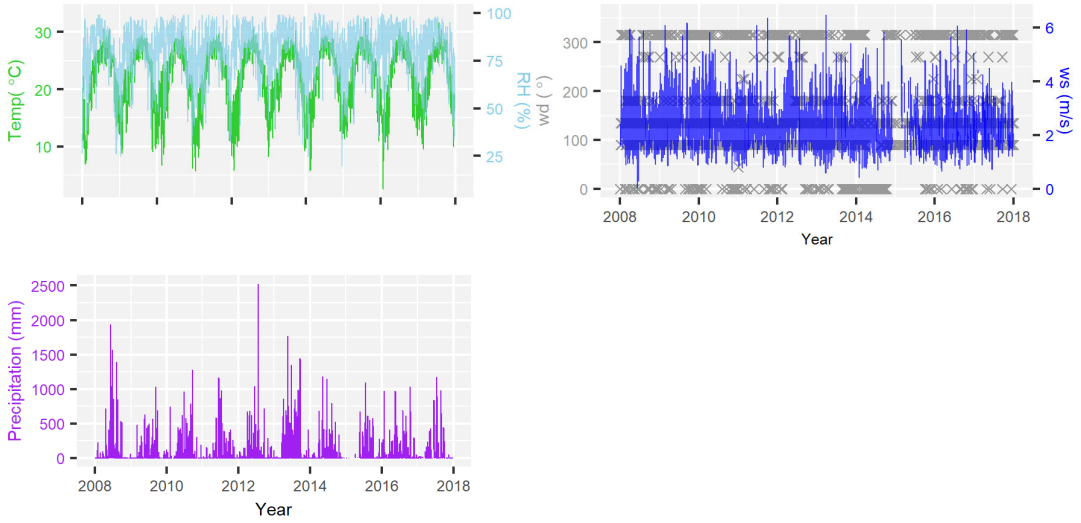

Figure S1 – Temperature and relative humidity (top-left), wind speed and direction (top-right), and precipitation (left-bottom) in Tsuen Wan from 2008 to 2017.

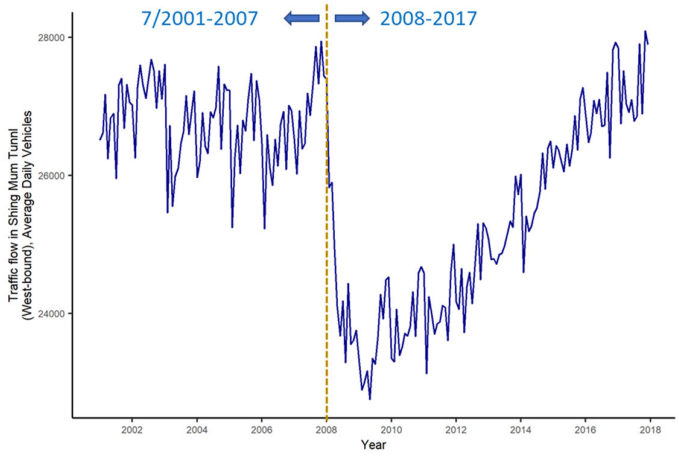

Figure S2 – Traffic flow counts in the Shing Mun Tunnel (West-bound: from Shatin to Tsuen Wan) from July 2001 to 2017. The sudden drop in traffic count in early 2008 coincided with the opening of the Eagle's Nest tunnel in March 2008, which likely had diverted traffic from the Shing Mun Tunnel.

S2. Supplemental figures related to $PM_{2.5}$ chemical composition data

The time series of individual samples are shown in Figure S3. The time series of seasonal averages for all the four seasons are shown in Figure S4.

One method to test whether the sample population is normally distributed is quartile-quartile plot (Q-Q plot). The concentration of species was first ranked in the increasing order and then the respective z-value in the normal distribution (e.g., the theoretical quartile of mean is 0) was calculated. If a linear relationship is observed from concentration versus the theoretical quartile, the sample population is normally distributed. For our sample population, a curve instead of a straight line was obtained in the Q-Q plots (Figure S5). The Q-Q plots were improved with the log transformation of the sample data (Figure S6). Thus, the log transformed time series were used for the trend analysis.

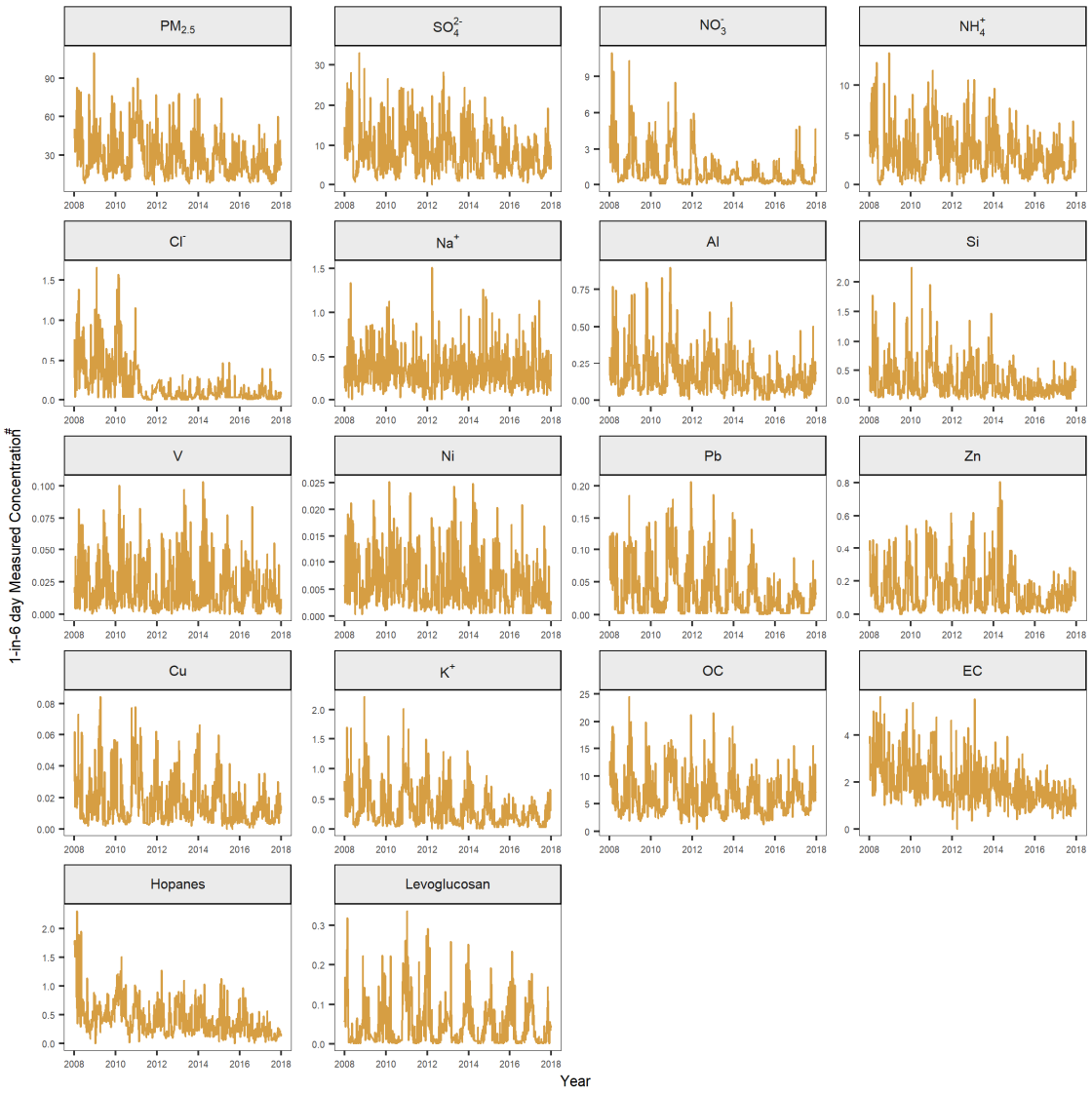

Figure S3 – Time series of individual samples collected in the decade of 2008-2017. #The concentration unit for hopanes is ng m^{-3}, while the unit for the other species is µg m^{-3}.

(a)

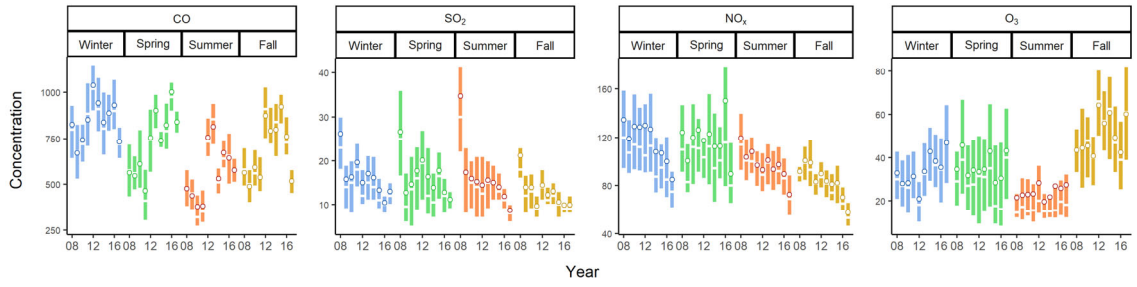

(b)

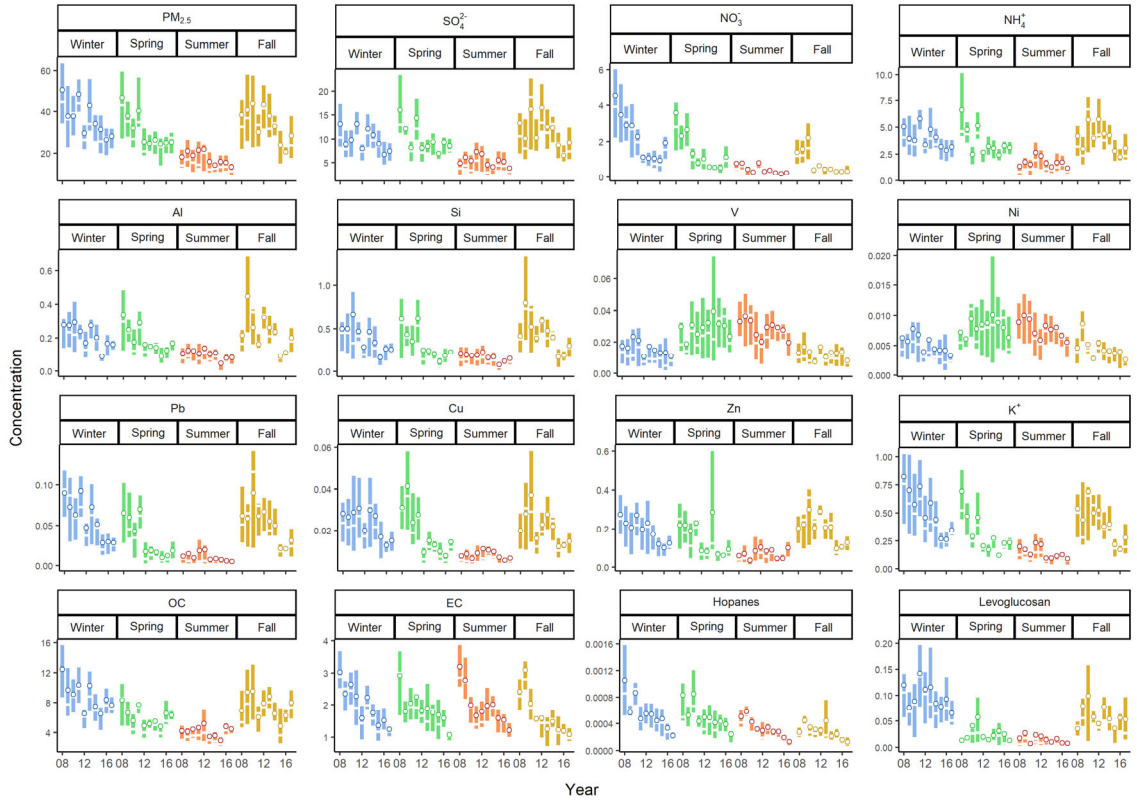

Figure S4 – Seasonal variations of (a) gaseous and (b) particle pollutants from 2008 to 2017. The concentration unit for all species is μg/m^3.

(a)

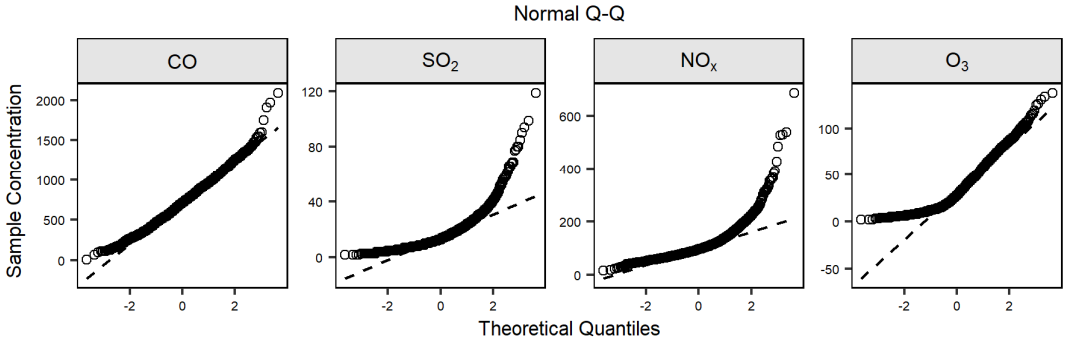

(b)

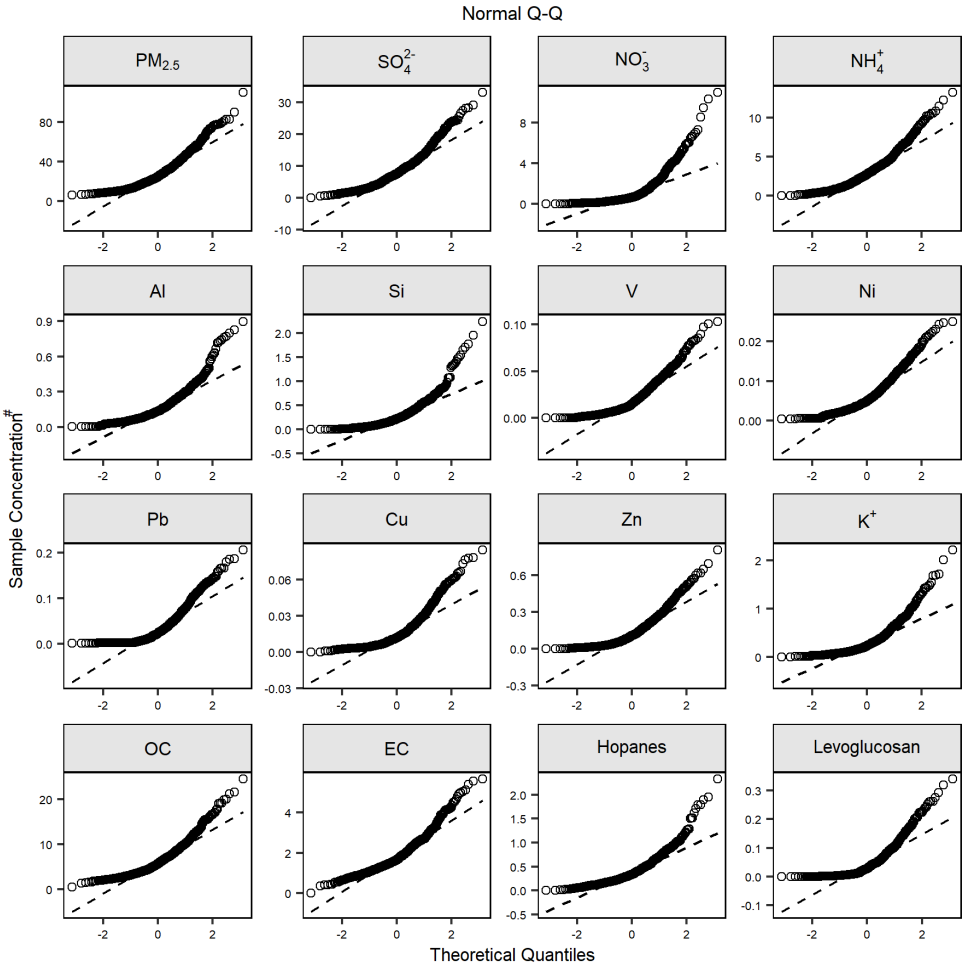

Figure S5 – QQ plots of (a) gaseous and (b) $PM_{2.5}$ species from 2008 to 2017. #The concentration unit for hopanes is ng/m^3 while the unit for the remaining species is µg/m^3. QQ plots (quantile-quantile plots) are used to examine whether the data are compatible with a certain distribution by comparing its sample quantiles against the theoretical quantiles. The closer the data points fall along the straight dash line in the figure, the more likely they are statistically distributed as per assumptions. Here we compare the raw data to a theoretical normal distribution for each species.

(a)

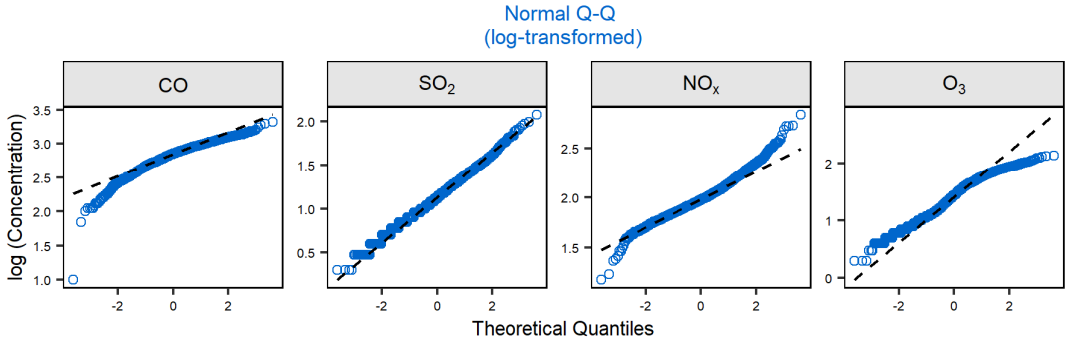

(b)

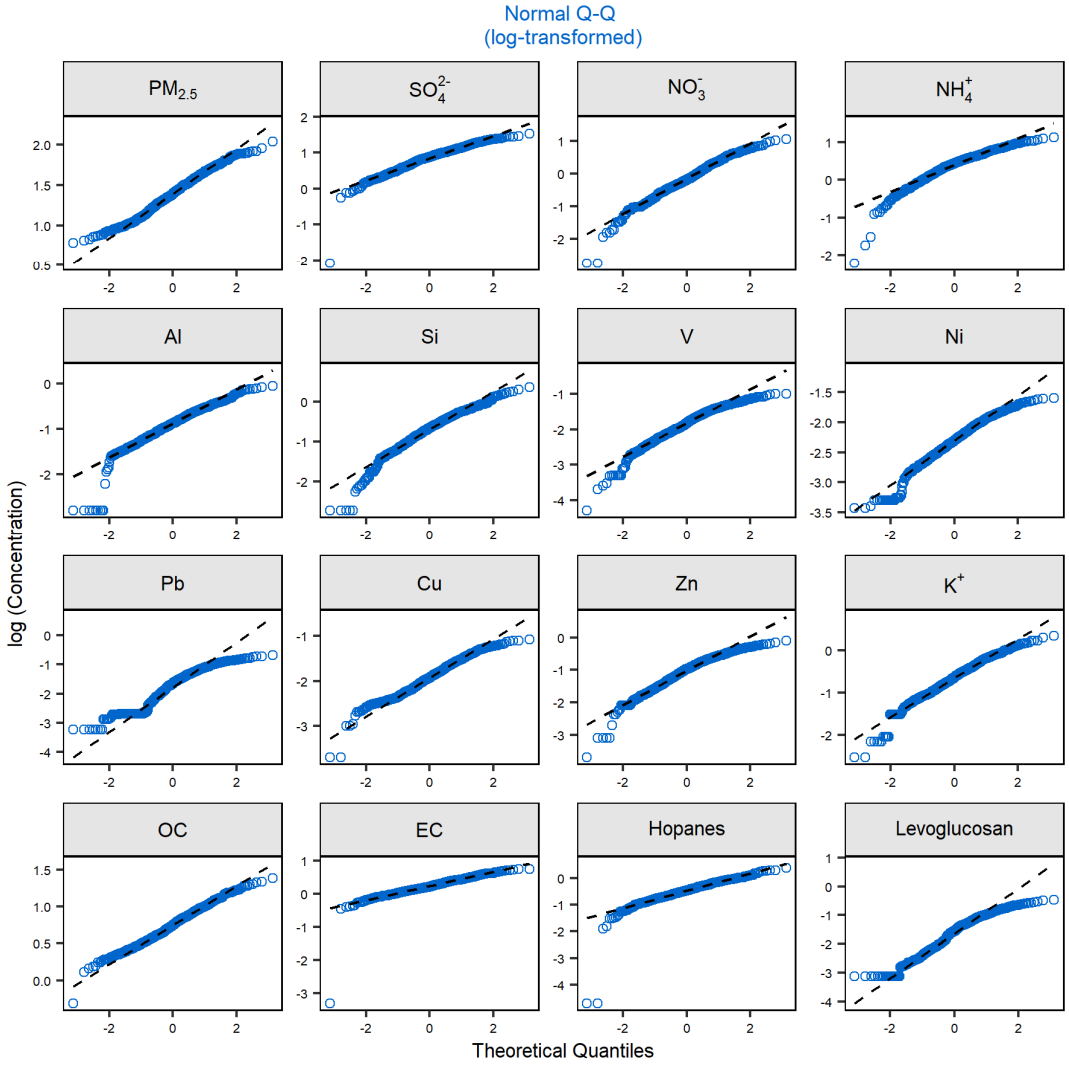

Figure S6 – QQ plots of (a) gaseous and (b) $PM_{2.5}$ species with log-transformation from 2008 to 2017. Note that the concentration unit for hopanes is ng/m^3 while the unit for the remaining species is µg/m^3.

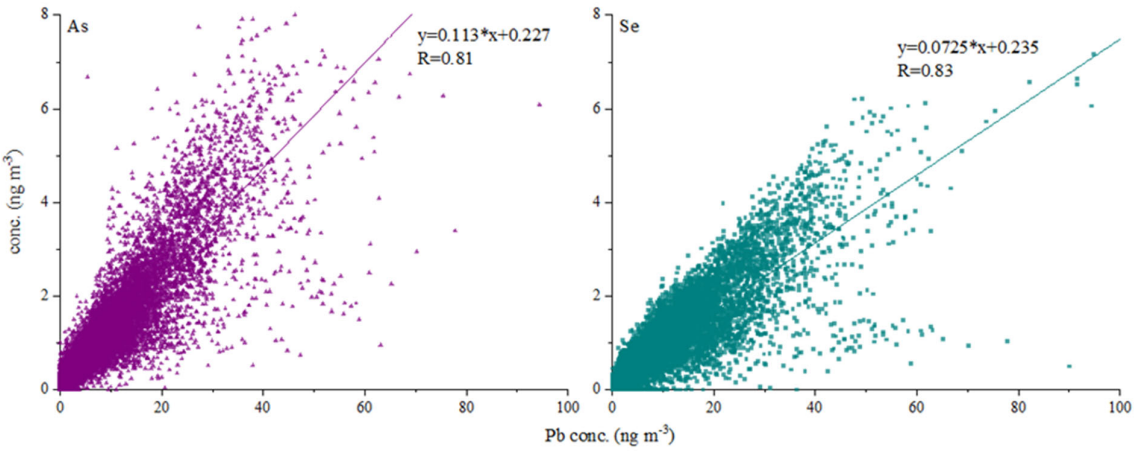

Figure S7 – Correlation of hourly concentrations of As and Se versus Pb at a suburban site of Hong Kong for the period of August 2019 - February 2021.

S3. Comparison of SO_2 emission inventories for Hong Kong and Guangdong and ambient SO_2 in Tsuen Wan, Hong Kong

As a criteria gaseous pollutant, SO_2 has been extensively studied and its emission inventories for Hong Kong and Guangdong province are available. We extracted the long-term emission inventories for Hong Kong and Guangdong from the HKEPD website (https://www.epd.gov.hk/epd/english/environmentinhk/air/data/emission_inve.html) and the MEIC data platform (version 1.3, http://meicmodel.org/?page_id=541&lang=en). The 10-year emission inventories of SO_2 are shown in Figure S8(a) for Guangdong and in Figure S8(b) for Hong Kong. The top two sources for SO_2 emissions in Hong Kong are power plants and marine vessels while the major SO_2 sources in Guangdong are power plants and industries. The emission and ambient concentration trends of SO_2, normalized against that in 2018, are examined in Figure S8c. The changes in the emissions from individual source sectors are shown in Figure S9 for both Guangdong and Hong Kong.

SO_2 in Guangdong began the decline in 2011 due to the significant drops of emissions from power plants and industrial sources (Figure S9a). In Hong Kong, there were obvious changes in emissions from public electricity generation (e.g., -28,500 tons in 2010; -9600 tons in 2015) and navigation sectors (e.g., -2,920 tons in 2016). The ten-year net reduction of SO_2 in Guangdong and in Hong Kong are -56% (from 1,091,400 to 480,100 tons) and -77% (from 694,700 to 16,170 tons), respectively.

The emission and ambient concentration trends of SO_2, normalized against that in 2018 (Figure S8c) show that the yearly variation of ambient SO_2 concentrations at TW was very similar to the total SO_2 emission trend from Hong Kong and SO_2 emission from power plants in Guangdong. Overall, the changes in ambient SO_2 concentrations at TW during the 10-year period are consistent with the SO_2 emissions estimated for the Greater Bay Area.

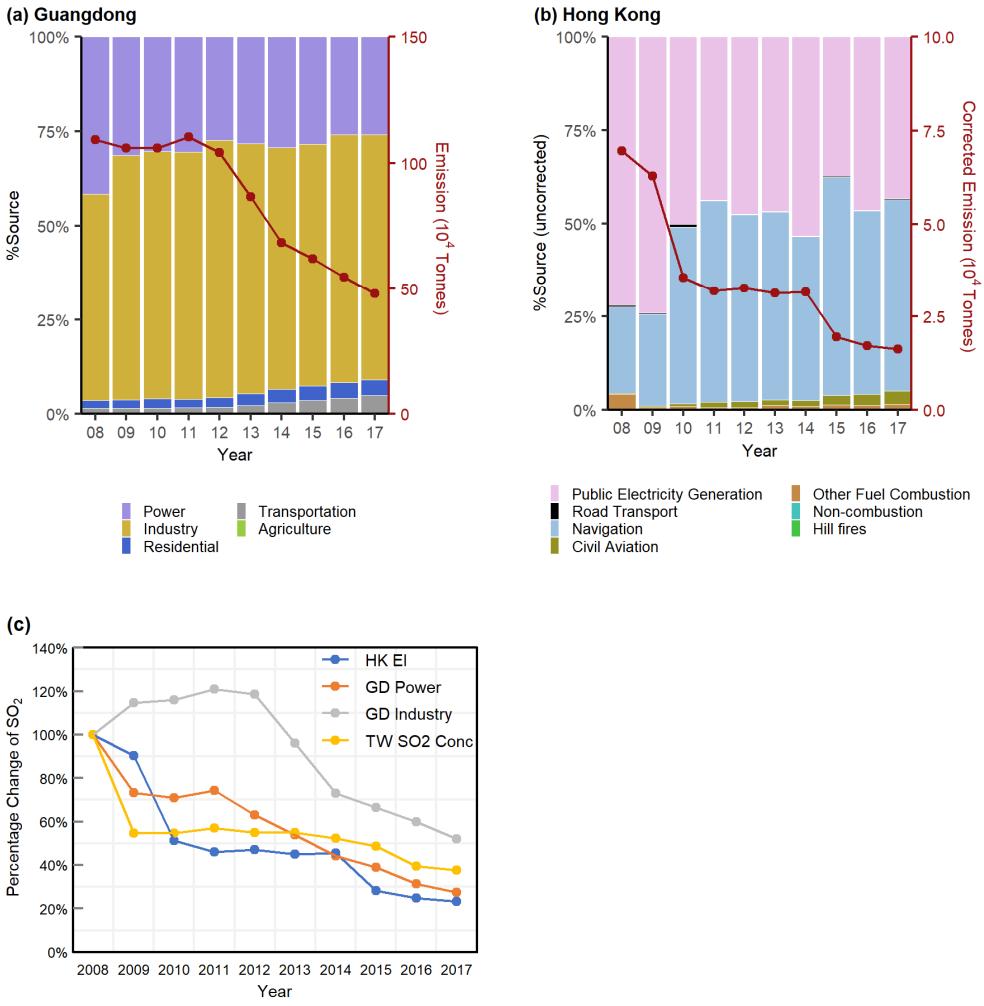

Figure S8 – Ten-year changes in percentage share of emissions by sources (columns) and variations in total SO_2 emissions (solid red line) in (a) Guangdong and (b) Hong Kong, with (c) comparing the ten-year trends of ambient SO_2 at TW and the major emission sources of SO_2 in Hong Kong (HK) and Guangdong (GD), HK EI indicates Public Electricity Genreation in Hong Kong.

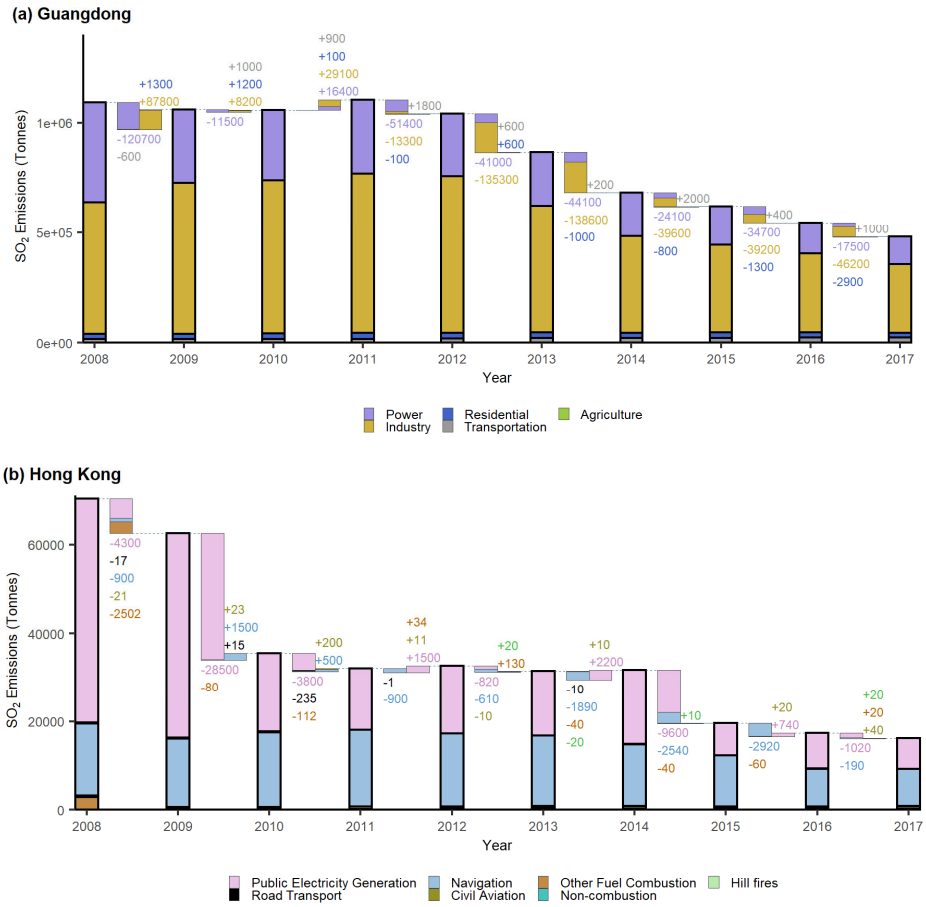

Figure S9 – Changes in the emissions from individual source sectors in (a) Guangdong and (b) Hong Kong. The small boxes and numbers between the columns indicate the annual changes in each year (left: negative value for decrement, right: positive value for increment).

S4. Methodology of Seasonal and Trend Decomposition with Loess Method (STL) and Generalized Least Squares with Autoregressive-Moving Average model (STL-GLS-ARMA)

The Seasonal and Trend Decomposition can be operated in either additional or multiplicative relationship as shown in equations 1a and 1b.

$$Y_v = T_v + S_v + R_v \quad (1a)$$

$$Y_v = T_v \times S_v \times R_v \quad (1b)$$

Eq (1b) can also be written as:

$$\log(Y_v) = \log(T_v) + \log(S_v) + \log(R_v); Y'_v = T'_v + S'_v + R'_v \quad (1c)$$

where *Yv, Tv, Sv, Rv* are the output data, the trend, the seasonal and the remainder component respectively, for *v* = 1 to N.

STL is optimized via locally weighted regression (typically the method LOcally Estimated Scatterplot Smoothing, LOESS) with weights $\boldsymbol{\theta_v}$ under two iterative loops, an inner loop nested inside an outer loop. Within the inner loop, the time series is first detrended with an initially estimated trend component. Then, the detrended time series is smoothed by LOESS with the smoothing parameter for seasonal component n_s and d = 1 under each cycle-subseries (e.g., January is the first cycle-subseries for the monthly cycles):

$$\text{Step 1: } Y_v^{detrend} = Y_v - T_v^k \text{ , } k \textit{ is the order of run in the inner loop} \quad (2)$$

$$\text{Step 2: } C_v^{k+1} \textit{ as smoothed sub} - \textit{cycle results from } Y_v^{detrend} \quad (3)$$

The third step in the inner loop is to compute a low-pass filter L_v^{k+1} from the locally weighted regression on three consecutive averaging means, which is later subtracted from the smoothed detrend sub-cycle results C_v^{k+1} (obtained from Step 2) so that a new seasonal component S_v^{k+1} is received.

$$\text{Step 3: } L_v^{k+1}, \textit{as low} - \textit{pass filter} \quad (4)$$

$$\text{Step 4: } S_v^{k+1} = C_v^{k+1} - L_v^{k+1} \quad (5)$$

A new trend component T_v^{k+1} is deduced after deseasonalizing the time series with the new seasonal component S_v^{k+1} and performing LOESS with the smoothing parameter for the trend component n_t and d=1.

$$\text{Step 5: } Y_v^{deseason} = Y_v - S_v^{k+1} \quad (6)$$

$$\text{Step 6: } T_v^{k+1}, \textit{as smoothed trend from } Y_v^{deseason} \quad (7)$$

After obtaining S_v^{k+1} and T_v^{k+1} from the inner loop, the remainder R_v can be calculated as shown in equation (8) in the outer loop, whence a robustness weight ρ_v is computed with respect to the R_v value. The inner loop is then repeated with the revised smoothing procedure including multiplication of ρ_v to the weights θ_v in Loess in Step 2 to Step 6 of the inner loop. The iterations of the inner and outer loop are carried out for a total of n_i and n_o times.

$$R_v = Y_v - T_v^{k+1} - S_v^{k+1} \quad (8)$$

$$\rho_v = B(|R_v|h) \quad (9.1)$$

Where *h* and *B*(*u*) are defined by the following two equations:

$$h = 6\, median(|R_v|) \quad (9.2)$$

$$B(u) = \begin{cases} (1-u^2)^2, & 0 \le u < 1 \\ 0, & u \ge 1 \end{cases} \quad (9.3)$$

After the STL method, generalized least squares with the ARMA model is carried out for quantifying the trend components of the time series. In the ARMA(*p,q*) model, it is assumed that the current value (X_t) is influenced by its *p*-order of lagged values (X_{t-h}) and *q*-order of lagged residuals (ε_{t-i}) as shown in equation 10.

$$X_t = \sum_{h=1}^{p} \phi_h X_{t-h} + \varepsilon_t + \sum_{i=1}^{q} \theta_i \varepsilon_{t-i} \quad (10)$$

Prior to running the model, the autocorrelation issue on the time series was examined by the Auto Correlation Function (ACF) and Partial ACF (PACF) by visually inspecting Figures S10 & S11. If the calculated ACF/PACF exceed the threshold (blue dotted line), then this indicates the time series to be autocorrelated. In our results, obvious autocorrelation with lagged values is observed for gaseous pollutants while autocorrelation of particle pollutants is higher with lagged residual (e.g., OC, EC, hopanes, etc.). After confirming the autocorrelation properties of the samples, order selection (*p, q values*) of the ARMA(*p,q*) model can be achieved by minimizing penalized model selection criteria such as Akaike's information criterion (AIC), AIC bias corrected (AICc), and Bayesian information criterion (BIC) (Table S1). Both AIC and BIC can quantify the overall influence of the increasing order on likelihood and overfitting issue of a model. AIC assumes that a model can only optimally predict the results, whilst BIC considers a model as the true model only when it generates the observed data. Despite the differences in assumptions, whichever model possesses the minimum AIC or BIC value is regarded as the most optimal. As AICc is the more restricted version of AIC, i.e., higher penalty applied with increasing order, AICc and AIC always align in the same sequence along the changes of the model order. Thus, any model selected by minimum AIC/AICc was denoted as "AIC selected model" in the table. In our results, 10 out of 20 species are optimized in different ARMA models if using different selection criteria. Only slight changes on the significant level of SO_4^- and NH_4^+ are observed while the determined slope by order selection does not show discernable variations among the models.

(a)

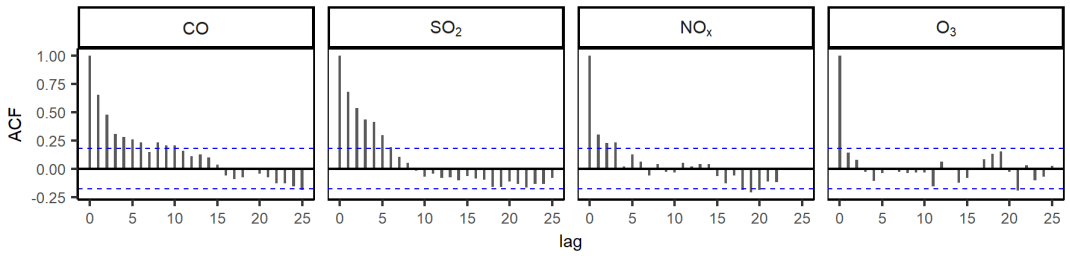

(b)

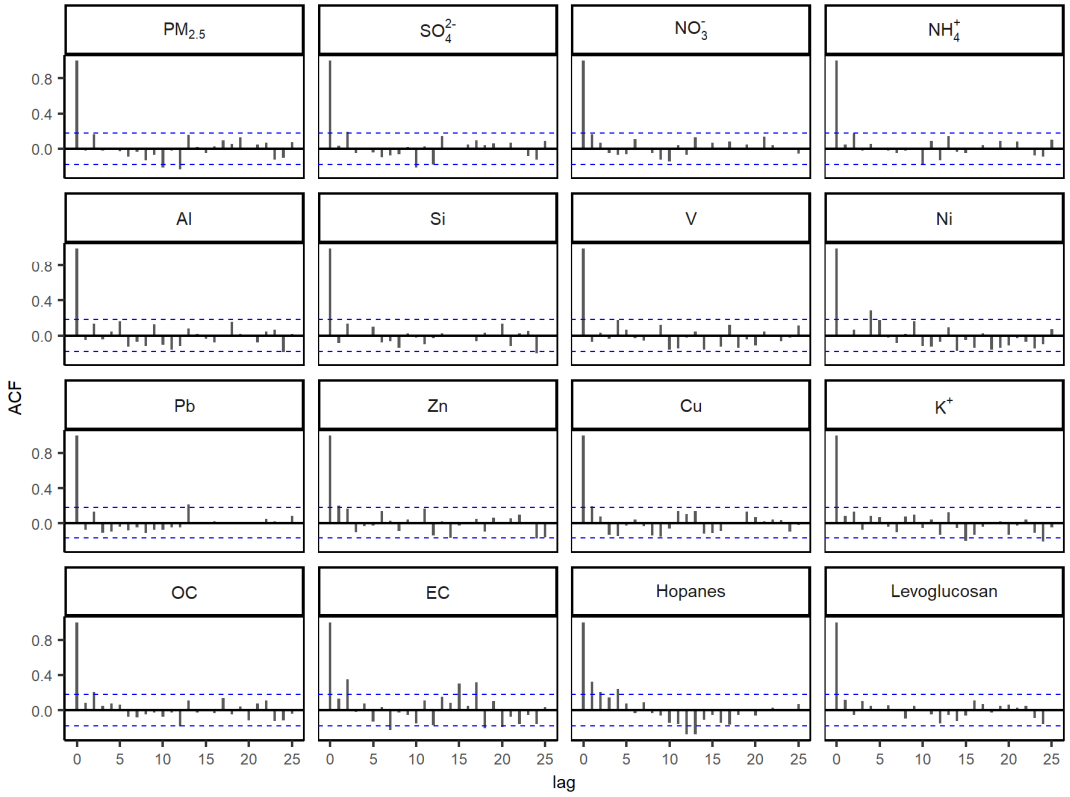

Figure S10 – ACF plots of (a) gaseous and (b) particle pollutants.

(a)

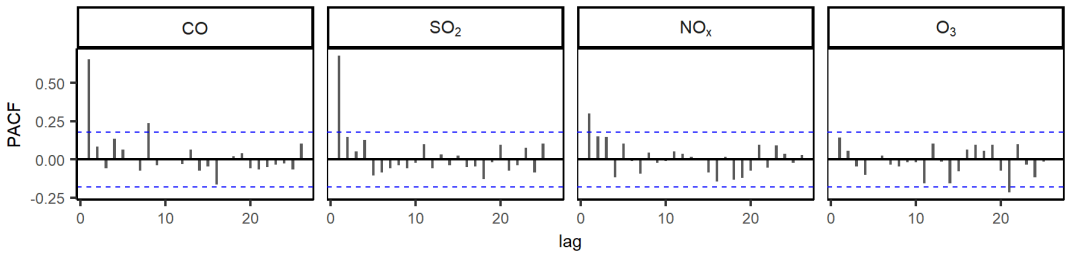

(b)

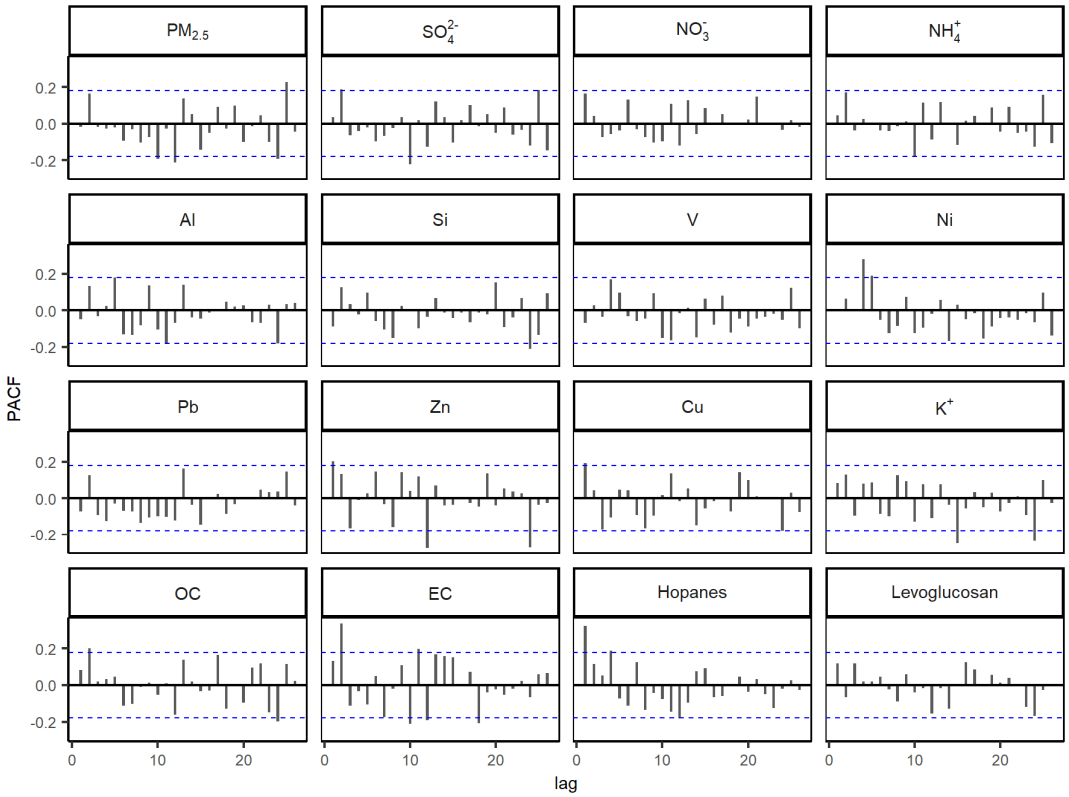

200 **Figure S11** –PACF plots of (a) gaseous and (b) particle pollutants.

Table S1. Summary of the ARMA model results, including minimum values among the information criteria, the respective selected model, exact value of the information criteria, slope, and the significance level determined from the model.

Species	Min. IC[1]	ARMA model	AIC	AICc	BIC	Slope[2]	Significance[3]	Slope Diff[4]
Gaseous pollutants								
CO	All	ARMR(1,0)	1481.7	1482	1492.8	20		*n.a.*
SO_2	AIC	ARMR(1,1)	607.4	607.9	621.3	-1.2	***	3.28×10^{-02}
	BIC	ARMR(1,0)	609.3	609.6	620.4	-1.2	***	
NO_x	AIC	ARMR(1,1)	942.7	943.2	956.6	-3.6	***	1.06×10^{-01}
	BIC	ARMR(1,0)	944.7	945.1	955.9	-3.5	***	
O_3	All	ARMR(1,0)	822.9	823.3	834.1	0.95	***	*n.a.*
Particle pollutants								
$PM_{2.5}$	AIC	ARMR(2,0)	818.4	818.9	832.3	-1.5	***	1.06×10^{-03}
	BIC	ARMR(1,0)	819.6	820	830.8	-1.5	***	
SO_4^{2-}	AIC	ARMR(0,2)	602.3	602.8	616.2	-0.36	**	2.45×10^{-04}
	BIC	ARMR(1,0)	604.9	605.2	616	-0.36	***	
NO_3^-	All	ARMR(1,0)	234.6	235	245.8	-0.16	***	*n.a.*
NH_4^+	AIC	ARMR(2,0)	402.3	402.8	416.2	-0.12	*	2.62×10^{-04}
	BIC	ARMR(1,0)	403.9	404.2	415	-0.12	**	
Al	AIC	ARMR(2,2)	-277.3	-276.3	-257.8	-13	***	9.06×10^{-02}
	BIC	ARMR(1,0)	-273.1	-272.8	-262	-13	***	
Si	All	ARMR(1,0)	-115.4	-115.1	-104.3	-27	***	*n.a.*
V	All	ARMR(1,0)	-814.5	-814.2	-803.4	-0.62	**	*n.a.*
Ni	All	ARMR(1,0)	-1130.9	-1130.5	-1119.7	-0.29	***	*n.a.*
Pb	AIC	ARMR(0,2)	-538.4	-537.9	-524.5	-3.8	***	1.28×10^{-02}
	BIC	ARMR(1,0)	-538.4	-538	-527.2	-3.9	***	
Zn	All	ARMR(2,2)	-329.2	-328.2	-309.7	-7.4	**	*n.a.*
Cu	AIC	ARMR(2,2)	-844.5	-843.5	-825	-1.1	***	2.80×10^{-03}
	BIC	ARMR(1,0)	-841	-840.7	-829.9	-1.1	***	
K^+	AIC	ARMR(2,2)	-133.9	-132.9	-114.3	-32	***	3.98×10^{-02}
	BIC	ARMR(1,0)	-131.7	-131.4	-120.6	-32	***	
OC	All	ARMR(2,0)	462.5	463	476.4	-0.18	**	*n.a.*
EC	All	ARMR(0,2)	133.9	134.4	147.8	-0.16	***	*n.a.*
Hopanes	AIC	ARMR(1,1)	-1790.3	-1789.7	-1776.3	-0.047	***	2.60×10^{-03}
	BIC	ARMR(1,0)	-1788.8	-1788.5	-1777.7	-0.044	***	
Levoglucosan	All	ARMR(0,1)	-586	-585.6	-575	-1.4	*	*n.a.*

[1] AIC = both AIC and AICc

[2] The unit for Al, Si, V, Ni, Pb, Zn, Cu, K^+, hopanes, and levoglucosan is ng $m^{-3}yr^{-1}$ while the unit is μg $m^{-3}yr^{-1}$ for the other species.

[3] Asterisks denotes that the significance of the slope differs from zero: * $p < 0.05$, ** $p < 0.01$, *** $p < 0.001$.

[4] Slope difference = |Slope 1 – Slope 2|; "n.a." denotes not applicable.

S5. Application of ordinary least square (OLS) and annual averaging on autocorrelated time series

After extracting the trend component by the STL method, OLS instead of the GLS-ARMA method is applied in this section for comparison purpose. The slope and the significant level estimated from both methods are almost the same, except for CO where a significant rise is obtained at 25 μg/m^3 per year (Table S2). Generally, the residual plots from the OLS methods (Figure S12) are less randomly distributed and more fluctuated (e.g., CO, SO_2, K^+, and NO_3^-). This reveals the importance of validating quantification methods on temporal variation in which the random and constant variance assumptions of OLS is proved incorrect in this study.

Concentrations estimated by the GLS-ARMA results are found generally smaller than the annual averaged values. The %Changes of species values are not different among the methods in situations of similar discrepancies in initial (Year, 2008) and end points (Year, 2017) (Table S3). For the species with a lesser decline rate in later years, such as K^+, NO_3^-, Al, Si, Pb and Cu, the determined slope from GLS-ARMA is dominated by the reduction during the first continuous decline period, and this leads to underestimated concentrations in 2017. The %difference of estimated concentration in 2017 ranges from -69.2% to 18.2% whereas the %difference in 2008 is generally smaller with -32.8% to 8.7%. Consequently, the %changes of species by GLS-ARMA are higher than those from the annual averaged method. Apart from this issue, GLS-ARMA is a better method for trend quantification owing to the higher degree of freedom in the calculation.

Table S2. Summary of the slope and intercept values determined by the OLS and GLS-ARMA methods.

			Slope		Intercept	
Species	**unit**	**ARMA model**	**GLS-ARMA**[1]	**OLS**[1]	**GLS-ARMA**	**OLS**
Gaseous pollutants						
CO	μg m^{-3} yr^{-1}	ARMR(1,0)	20, (-0.84, 40)	25***, (15, 34)	590	570
SO_2	μg m^{-3} yr^{-1}	ARMR(1,0)	-1.2***, (-1.8, -0.65)	-1.2***, (-1.5, -0.96)	22	22
NO_x	μg m^{-3} yr^{-1}	ARMR(1,0)	-3.5***, (-4.6, -2.4)	-3.5***, (-4.3, -2.7)	120	120
O_3	μg m^{-3} yr^{-1}	ARMR(1,0)	0.95***, (0.42, 1.5)	0.93***, (0.47, 1.4)	28	28
Particle pollutants						
$PM_{2.5}$	μg m^{-3} yr^{-1}	ARMR(1,0)	-1.5***, (-1.9, -1.1)	-1.5***, (-2, -1.1)	35	35
SO_4^{2-}	μg m^{-3} yr^{-1}	ARMR(1,0)	-0.36***, (-0.55, -0.17)	-0.36***, (-0.54, -0.17)	10	10
NO_3^-	μg m^{-3} yr^{-1}	ARMR(1,0)	-0.16***, (-0.21, -0.12)	-0.17***, (-0.21, -0.13)	1.8	1.8
NH_4^+	μg m^{-3} yr^{-1}	ARMR(1,0)	-0.12**, (-0.21, -0.039)	-0.12**, (-0.2, -0.043)	3.6	3.6
Al	ng m^{-3} yr^{-1}	ARMR(1,0)	-13***, (-17, -8)	-13***, (-17, -7.8)	230	230
Si	ng m^{-3} yr^{-1}	ARMR(1,0)	-27***, (-36, -19)	-27***, (-36, -18)	420	420
V	ng m^{-3} yr^{-1}	ARMR(1,0)	-0.62**, (-1.1, -0.16)	-0.62*, (-1.1, -0.13)	23	23
Ni	ng m^{-3} yr^{-1}	ARMR(1,0)	-0.29***, (-0.43, -0.16)	-0.29***, (-0.43, -0.16)	7.6	7.6
Pb	ng m^{-3} yr^{-1}	ARMR(1,0)	-3.9***, (-5.3, -2.4)	-3.9***, (-5.4, -2.3)	49	49
Zn	ng m^{-3} yr^{-1}	ARMR(2,2)	-7.4**, (-12, -2.6)	-7.2***, (-11, -3.1)	170	160
Cu	ng m^{-3} yr^{-1}	ARMR(1,0)	-1.1***, (-1.7, -0.59)	-1.1***, (-1.6, -0.69)	21	21
K^+	ng m^{-3} yr^{-1}	ARMR(1,0)	-32***, (-41, -23)	-32***, (-41, -24)	460	460
OC	μg m^{-3} yr^{-1}	ARMR(2,0)	-0.18**, (-0.32, -0.047)	-0.18***, (-0.28, -0.075)	7.1	7.1
EC	μg m^{-3} yr^{-1}	ARMR(0,2)	-0.16***, (-0.2, -0.13)	-0.17***, (-0.19, -0.14)	2.7	2.7
Hopanes	ng m^{-3} yr^{-1}	ARMR(1,0)	-0.044***, (-0.057, -0.031)	-0.043***, (-0.052, -0.033)	0.62	0.61
Levoglucosan	ng m^{-3} yr^{-1}	ARMR(0,1)	-1.4*, (-2.7, -0.077)	-1, (-4.2, 2.2)	42	45

[1] Asterisks indicate the degree of statistical significance regarding whether the slope is significantly different from zero, with * denoting $p < 0.05$, ** denoting $p < 0.01$, and *** denoting $p < 0.001$.

(a)

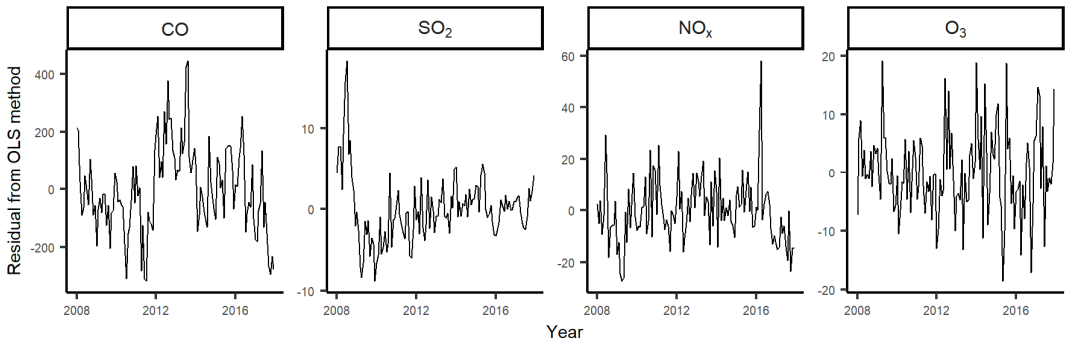

(b)

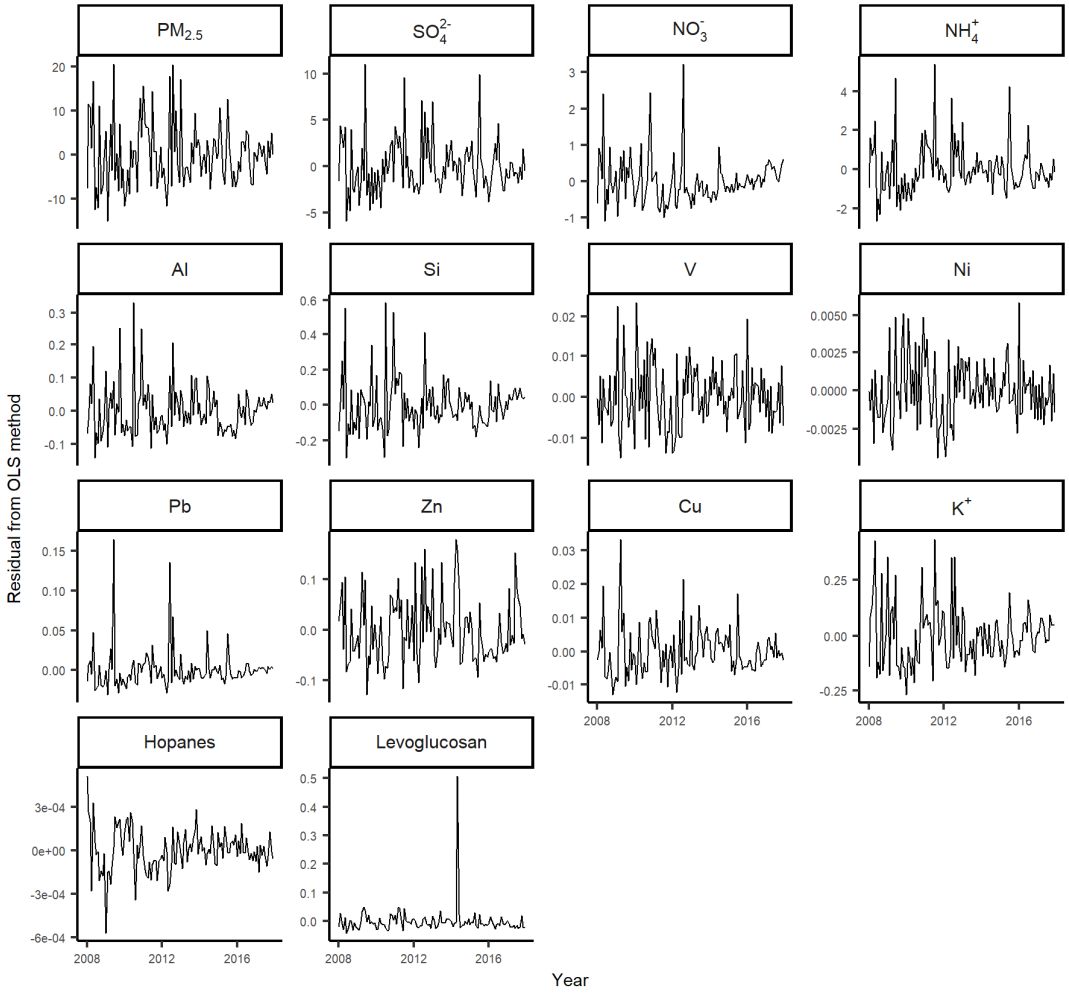

Figure S12 – Residual plots of the OLS method for (a) gaseous and (b) particle pollutants. Note that the residual unit for hopanes and levoglucosan is ng/m^3, while that for the remaining substances is in µg/m^3.

Table S3. Summary of the annual averaged concentrations and the estimated values by GLS-ARMA in 2008 and 2017.

		Concentration in 2008		Concentration in 2017		%Diff in methods[1]	
Species	**unit**	**GLS-ARMA**	**Annual averaged**	**GLS-ARMA**	**Annual averaged**	**2008**	**2017**
Gaseous pollutants							
CO	μg m^{-3}	610	620	780	660	-1.6%	18.2%
SO_2	μg m^{-3}	21	28	10	11	-25.0%	-9.1%
NO_x	μg m^{-3}	120	120	88	77	0.0%	14.3%
O_3	μg m^{-3}	28	31	37	42	-9.7%	-11.9%
Particle pollutants							
$PM_{2.5}$	μg m^{-3}	34	37	21	22	-8.1%	-4.5%
SO_4^{2-}	μg m^{-3}	9.8	11	6.6	6.6	-10.9%	0.0%
NO_3^-	μg m^{-3}	1.8	2.6	0.28	0.91	-30.8%	-69.2%
NH_4^+	μg m^{-3}	3.5	4	2.4	2.4	-12.5%	0.0%
Al	ng m^{-3}	220	220	110	140	0.0%	-21.4%
Si	ng m^{-3}	410	410	160	220	0.0%	-27.3%
V	ng m^{-3}	23	24	17	16	-4.2%	6.3%
Ni	ng m^{-3}	7.5	6.9	4.8	4.5	8.7%	6.7%
Pb	ng m^{-3}	47	57	12	19	-17.5%	-36.8%
Zn	ng m^{-3}	160	190	96	110	-15.8%	-12.7%
Cu	ng m^{-3}	21	21	10	12	0.0%	-16.7%
K^+	ng m^{-3}	440	560	160	220	-21.4%	-27.3%
OC	μgC m^{-3}	7	8.2	5.4	6.3	-14.6%	-14.3%
EC	μgC m^{-3}	2.7	2.9	1.2	1.2	-6.9%	0.0%
Hopanes	ng m^{-3}	0.60	0.71	0.21	0.18	-15.5%	16.7%
Levoglucosan	ng m^{-3}	41	61	29	33	-32.8%	-12.1%

[1] Percent difference is the relative difference of t**he** concentrations estimated by two methods [(GLS-ARMA - Annual averaged) ÷ Annual method x 100%]

230

S6. Trend determination with different time intervals

From the STL trend component and the different %changes in the annual averaged and the GLS-ARMA methods, the time series of some species are found not always monotonically decreasing. To study the exact period of decline in certain species (K^+, NO_3^-, Al, Si, V, Ni, Pb, Zn, and Cu), five additional time intervals (2008-2016, 2008-2015, 2008-2014, 2014-2017 & 2015-2017) were analyzed with the STL-GLS-ARMA method (Table S4). For the reference species EC with a consistent decline from 2008-2017, the slope and intercept remained nearly unchanged in all time intervals. On the contrast, the changes of slope and intercept among time intervals before and after 2014 were significant for the remaining species. For K^+ and NO_3^-, the reduction increased when data from 2015-2017 (i.e., only include 2008-2014) were removed; no significant trend was observed in the time intervals of 2014/2015-2017, showing that the decline was stronger in early state and was getting flattened in later years. The declines of Al and Si were also weaker in later years and even a rise was noted in the 2015-2017 period while the temporal variations of industrial tracers Pb, Zn and Cu were relatively stable in the earlier period with weaker decline starting from 2015. The situation was opposite for ship emission-sourced V and Ni where a significant and stronger reduction was obtained after 2015, possibly owing to the implementation of policy in 2015 which requires marine vessels to switch to clean fuels in Hong Kong waters.

Table S4. Summary of slopes and intercepts (in parentheses) for time series spanning different time intervals.

	Slope[1] (Intercept) in different time intervals					
Species	**2008-2017**	**2008-2016**	**2008-2015**	**2008-2014**	**2014-2017**	**2015-2017**
EC	-0.16*** (2.7)	-0.16*** (2.7)	-0.18*** (2.8)	-0.18*** (2.8)	-0.18*** (2.9)	-0.14*** (2.6)
K^+	-32*** (460)	-35*** (470)	-38*** (480)	-36*** (470)	-14 (320)	-0.88 (200)
NO_3^-	-0.16*** (1.8)	-0.19*** (1.9)	-0.21*** (2)	-0.22*** (2)	-0.00035 (0.55)	0.055 (0.055)
Al	-13*** (230)	-14*** (230)	-15*** (230)	-8.5* (220)	-4.8 (160)	24 (-96)
Si	-27*** (420)	-31*** (430)	-33*** (440)	-25** (420)	-4 (230)	30 (-80)
Pb	-3.9*** (49)	-3.9*** (49)	-3.8** (48)	-3.3* (47)	-3.6* (46)	-1.9* (31)
Zn	-7.4** (170)	-9** (170)	-6.8 (160)	-1.8 (150)	-11 (190)	14 (-25)
Cu	-1.1*** (21)	-1.2*** (21)	-0.92* (21)	-0.62 (20)	-1.8* (27)	-0.79 (17)
V	-0.62** (23)	-0.42 (22)	-0.54 (23)	-0.49 (23)	-1.8** (33)	-2.1** (36)
Ni	-0.29*** (7.6)	-0.25** (7.4)	-0.26* (7.5)	-0.25 (7.4)	-0.54** (9.5)	-0.84*** (12)

[1]The unit for EC and NO_3^- is $\mu g\ m^{-3}\ yr^{-1}$ and that for other species is $ng\ m^{-3}\ yr^{-1}$. Asterisks denote that the slope values significantly different from zero: * $p < 0.05$, ** $p < 0.01$, *** $p < 0.001$.

S7. Overall compound annual average results (CAGR) of all species.

The table below shows the summary results adopting the CAGR method and comparison with the GLS-ARMA method. Figure S13 summarizes the CAGR results of all the pairwise combinations in each species over the ten years.

Table S5. Summary of the CAGR from annual averaged time series.

Species	%Relative change per year		
	CAGR	GLS-ARMA	Difference[1]
Gaseous pollutants			
CO	3.2%	3.3%	-0.1%
SO_2	-5.1%	-5.6%	0.5%
NO_x	-2.6%	-2.9%	0.3%
O_3	2.4%	3.5%	-1.1%
$PM_{2.5}$ and components			
$PM_{2.5}$	-5.7%	-4.3%	-1.4%
SO_4^{2-}	-5.1%	-3.6%	-1.5%
NO_3^-	-19%	-9.0%	-10%
NH_4^+	-4.4%	-3.4%	-1.0%
Al	-5.8%	-5.5%	-0.3%
Si	-9.0%	-6.5%	-2.5%
V	-2.8%	-2.7%	-0.1%
Ni	-4.8%	-3.9%	-0.9%
Pb	-13%	-7.9%	-5.1%
Zn	-7.1%	-4.5%	-2.6%
Cu	-8.0%	-5.4%	-2.6%
K^+	-11%	-7.0%	-4%
OC	-3.0%	-2.6%	-0.4%
EC	-8.4%	-6.0%	-2.4%
Hopanes	-12%	-7.1%	-4.9%
Levoglucosan	-4.9%	-3.3%	-1.6%

[1]Difference of percent relative change is calculated from the two methods (CAGR – GLS-ARMA)

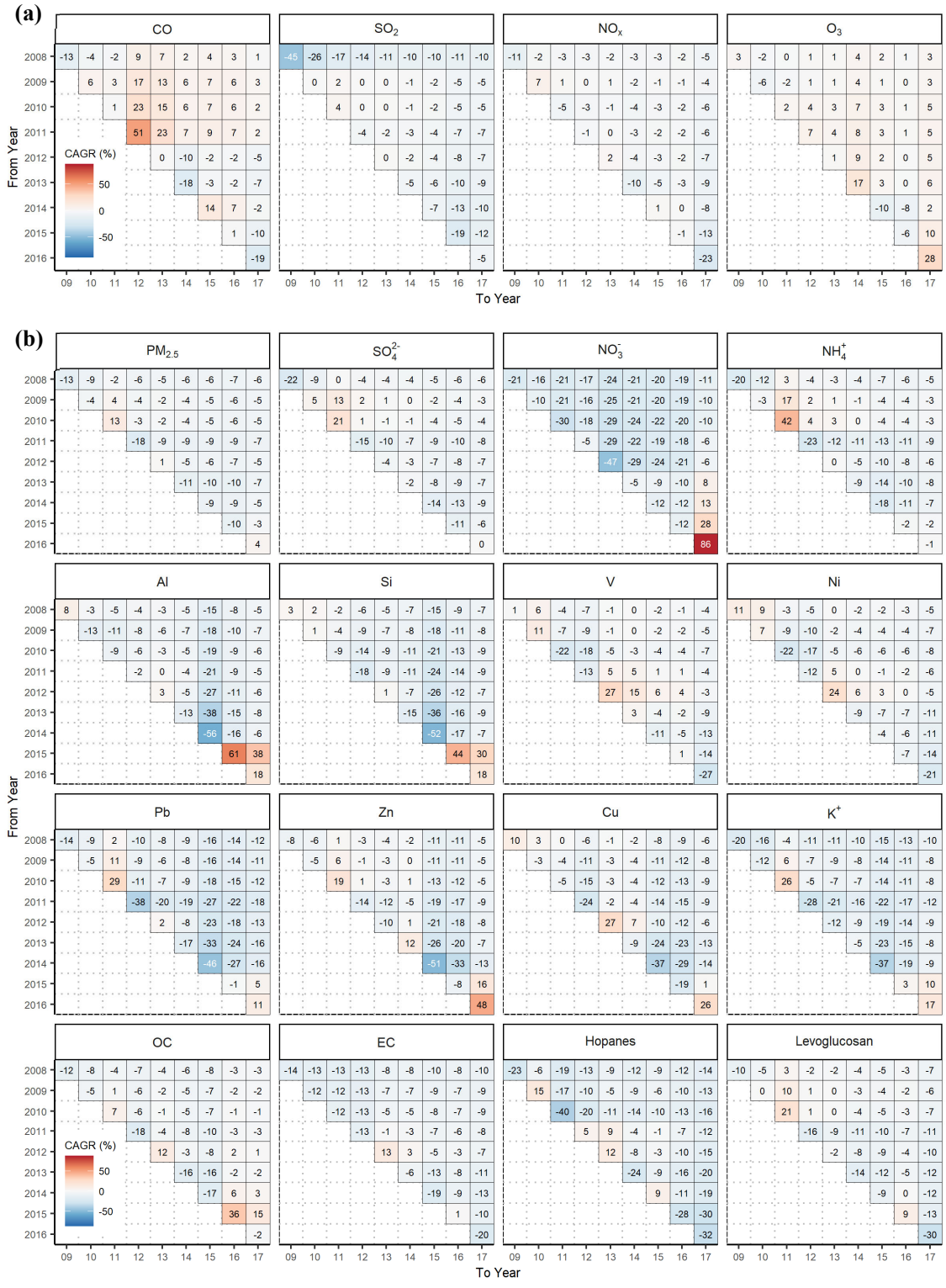

Figure S13 – CAGR of all pairwise combinations in each species from 2008 to 2017.

S8. El Niño-Southern Oscillation (ENSO) events

Occurrences of ENSO events are summarized in Table S6. The respective influences of ENSO events on wind components are summarized in Figure S14. The coefficients of all the variables in the multiple linear regression (MLR) equation (4) are summarized in Table S7 and Figure S15.

Table S6. Summary of ENSO events from 2008 to 2017 as neutral, weak, moderate, strong, and very strong events.

El Niño/La Niña event	Occurring period	Season	Strength
El Niño #1	08. 2009 – 10. 2009	Summer – Fall	Weak
	11. 2009 – 12. 2009	Winter – Winter	Moderate
	01. 2010 – 01. 2010	Winter – Winter	Strong
	02. 2010 – 03. 2010	Winter – Spring	Moderate
	04. 2010 – 05. 2010	Spring – Summer	Weak
El Niño #2	11. 2014 – 05. 2015	Winter – Summer	Weak
	06. 2015 – 07. 2015	Summer – Summer	Moderate
	08. 2015 – 09. 2015	Summer – Fall	Strong
	10. 2015 – 03. 2016	Fall – Spring	Very Strong
	04. 2016 – 04. 2016	Spring – Spring	Strong
	05. 2016 – 05. 2016	Summer – Summer	Moderate
LaNiña #1	01. 2008 – 01. 2008	Winter – Winter	Moderate
	02. 2008 – 03. 2008	Winter – Spring	Strong
	04. 2008 – 05. 2008	Spring – Summer	Moderate
	06. 2008 – 09. 2009	Summer – Fall	Weak
La Niña #2	08. 2010 – 08. 2010	Summer – Summer	Weak
	09. 2010 – 10. 2010	Fall – Fall	Moderate
	11. 2010 – 01. 2011	Winter – Winter	Strong
	02. 2011 – 03. 2011	Winter – Spring	Moderate
	04. 2011 – 06. 2011	Spring – Summer	Weak
	10. 2011 – 12. 2011	Fall – Winter	Weak
La Niña #3	02. 2012 – 02. 2012	Winter – Winter	Moderate
	03. 2012 – 04. 2012	Winter – Spring	Weak

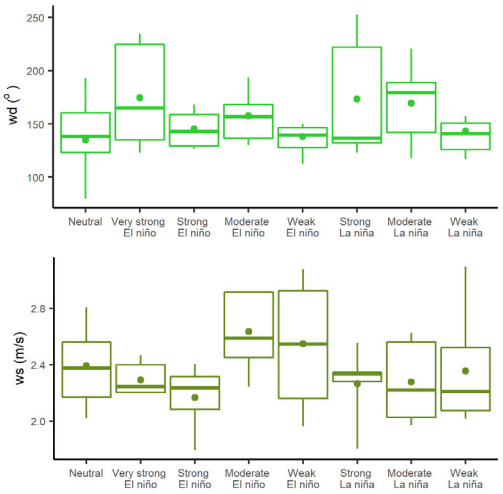

Figure S14 – Changes of wind direction (top) and wind speed (bottom) under different levels of ENSO events.

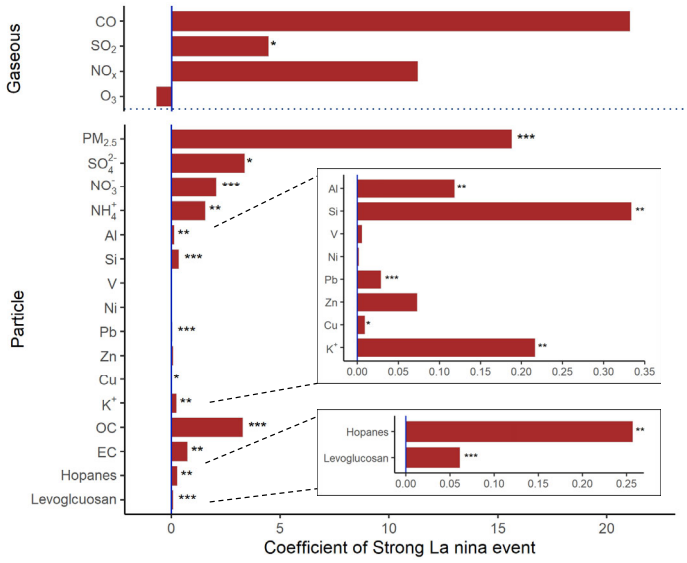

Figure S15 – Visual display of the coefficients of Strong La niña event for various gaseous (upper panel) and particle (bottom panel) species**.** The numerical values are listed in the column headed with "Strong La nina" in Table S7. Asterisks denote the coefficient of each variable significantly different from zero: * $p < 0.05$, ** $p < 0.01$, *** $p < 0.001$.

Table S7. Coefficient values of variables in the multiple linear regression Eq. (4).

Species	Coefficients[1]													
	Year	Spring[3]	Summer[3]	Fall[3]	Temp	RH	Very strong El Nino	Strong El Nino	Moderate El nino	Weak El Nino	Strong La Nina	Moderate La Nina	Weak La Nina	Intercept
Gaseous pollutants														
CO	**+21*** **	*+3.1*	*+21*	*+96*	**-35*** **	*+4.6*	*+35*	*+130*	*-12*	*-28*	*+21*	*-24*	*-46*	**+970*** **
SO_2	**-0.87*** **	*+2.1*	*+4.2*	*+0.059*	*-0.2*	*-0.08*	*-1.9*	*-0.64*	*-1.4*	*+0.53*	**+4.4***	**+3.9***	**+4** **	**+29*** **
NO_x	**-3.1*** **	**+17*** **	**+14***	*-0.35*	**-3.3*** **	**+0.62***	*+3.4*	**+21** **	*+2.7*	*+4.9*	*+11*	**+13***	*+3.6*	**+130*** **
O_3	**+1.2*** **	**+6.8***	*-3.8*	**+13** **	*+0.36*	**-0.92*** **	*-0.39*	*-2.5*	*-3.1*	*+0.83*	*-0.69*	*-1.8*	*-1.6*	**+92*** **
Particle pollutants														
$PM_{2.5}$	**-0.93*** **	**+6.5** **	*+1.1*	**+7.3***	**-0.82***	**-0.77*** **	*-4.3*	*-0.35*	*+1*	*+1.9*	**+16*** **	*+4.6*	*-2.2*	**+110*** **
SO_4^{2-}	*-0.19*	**+2.8** **	*+0.16*	**+3.9** **	*-0.14*	**-0.2*** **	*-1.8*	*+0.027*	*+0.69*	*+0.23*	**+3.4***	**+2.8***	*-0.32*	**+28*** **
NO_3^-	**-0.16*** **	**+0.58***	*+0.51*	*+0.24*	**-0.15*** **	*-0.021*	*-0.22*	*+0.078*	*+0.38*	*-0.19*	**+2.1*** **	**+0.76** **	**-0.64** **	**+6.9*** **
NH_4^+	*-0.06*	**+0.97** **	*+0.39*	**+1.5** **	**-0.15** **	**-0.071*** **	*-0.86*	*-0.14*	*-0.063*	*-0.3*	**+1.6** **	**+1.2** **	*-0.22*	**+12*** **
Al^2	**-10*** **	*+50*	*-35*	*+15*	*+3.3*	**-7*** **	*-31*	*-49*	*-14*	*-0.59*	**+120** **	*+13*	**-51***	**+730*** **
Si^2	**-19** **	*+96*	*-54*	*+8.5*	*+9.7*	**-17*** **	*-37*	*+34*	*-1.5*	*+18*	**+330*** **	*+56*	*-52*	**+1500*** **
V^2	**-0.71***	**+16*** **	**+14** **	*+3.3*	*-0.051*	*+0.31*	*-1.8*	*-0.15*	*+3.8*	*+1.3*	*+5.6*	*+0.57*	*-4*	*-6.3*
Ni^2	**-0.29** **	**+4.1*** **	**+3.4** **	*+1*	*-0.031*	*+0.057*	*-0.1*	*+0.48*	*+1.7*	*+0.77*	*+1.7*	*+0.32*	*-1*	*+1.9*
Pb^2	**-2.7*** **	*+3.1*	*-4.6*	*+7.7*	*-1.1*	**-2.3*** **	*-13*	*-0.34*	*+3.7*	*-2.7*	**+29*** **	**+16***	*-1.1*	**+260*** **
Zn^2	*-5.3*	*+29*	*-39*	*+7.9*	*-0.56*	**-6.1*** **	*-57*	*-33*	*-3.4*	*-11*	*+73*	*+34*	*-20*	**+690*** **
Cu^2	**-0.8** **	*+4.6*	*-0.47*	*+2.7*	*-0.43*	**-0.71*** **	*-4.3*	*-0.56*	*+0.46*	*+1.7*	**+8.9***	*+5.6*	*-4.1*	**+87*** **
K^{+2}	**-27*** **	*-23*	*-82*	*-6.4*	*-11*	**-13*** **	*-110*	*-68*	*-9.2*	**-97***	**+220** **	*+73*	*-45*	**+1800*** **
OC	*-0.079*	*+0.27*	*-0.77*	*+0.088*	*-0.11*	**-0.21*** **	*-0.55*	*-0.33*	*-0.21*	*-0.39*	**+3.3*** **	*+0.66*	*-0.78*	**+26*** **
EC	**-0.15*** **	*+0.19*	*+0.31*	*-0.025*	*+0.0003*	*-0.0091*	*+0.02*	*+0.14*	*+0.088*	*+0.22*	**+0.74** **	*+0.067*	*-0.029*	**+3.3*** **
Hopanes[2]	**-0.045*** **	*0.069*	*0.012*	*-0.078*	**-0.022***	**0.0069***	*0.011*	*0.17*	*0.13*	*0.088*	**0.26** **	*0.051*	*-0.071*	**0.57***
Levoglucosan[2]	*+0.64*	**-32*** **	*-12*	*-4.1*	**-4.6*** **	**-1.9*** **	*+8.6*	*-6.5*	*+5.8*	*+7.4*	**+61*** **	*+12*	*+7.6*	**+310*** **

[1]Asterisks denote the coefficient of each variable significantly different from zero: * $p < 0.05$, ** $p < 0.01$, *** $p < 0.001$. Coefficients significantly different from zero are in bold.
[2]The concentration unit for hopanes is ng/m^3 and the unit for the other species is μg/m^3.
[3] As season is a categorical variable, when estimating the coefficients for the seasons in the MLR, one season needs to act as the reference variable. Here winter is used as the reference variable for estimating the coefficients of the other three seasons, thus no coefficient is calculated for the winter season.

S9. Emissions control policies implemented in Hong Kong and in the Pearl River Delta (PRD)

Table S8. Summary of local and joint-government regulations/policies in Hong Kong under Air Pollution Control Ordinance and in the Pearl River Delta under Guangdong Action Plan and related regulations.

Type of emission	Effective region[1]	Issue Year	Descriptions	Remarks (if any)
Vehicles[2]	Hong Kong (HK)	2007	Replace pre-Euro & Euro I Diesel Commercial Vehicles (DCVs)	
		2010	Replace Euro II DCVs	By 30th June 2013
		2010	Tighten diesel and unleaded petrol vehicle to Euro V standard	
		2011	The Statutory Ban – forbidden the stationary vehicles from operating engine for more than 3 minutes in any continuous 60 min period	
		2012	Euro V emission standards for all newly registered vehicles	
		2013	Voluntary replacement of catalytic converters and oxygen sensors on LPG vehicles	Completed in April 2014; about 13,900 taxis and 2,900 light buses involved
		2014	Strengthen emission control for petrol and LPG vehicle	
		2014	Phasing out pre-Euro IV DCVs	~ 82,000 DCVs phased out
		2015	Trials on electric buses implement	
		2015	Set up franchised bus low emission zone in Causeway Bay, Central and Mong Kok	
		2017	Euro VI emission standards for all newly registered vehicles	
		2020	Phasing out Euro IV DCVs	By the end of 2027
		2021 *(Proposed)*	Tighten emission standards of first registered motorcycles, light buses and buses	
	China	2007	China III emission standards for (1) light-duty vehicles & (2) compression ignition and gas fueled positive ignition engines	
		2009	China III emission standards for heavy-duty vehicles	
		2010	China IV emission standards for (1) light-duty vehicles & (2) compression ignition and gas fueled positive ignition engines	
		2012	China IV emission standards for heavy-duty vehicles	
		2012	China V emission standards for compression ignition and gas fuelled positive ignition engines	
		2014	Eliminate the “yellow-label” car in Guangdong Province (GD)	By the end of 2017

Vehicles (Cont'd)	China	2015	China V emission standards for (1) light-duty vehicles; (2) light gasoline, light diesel & heavy diesel vehicles	Heavy diesel vehicles including buses, sanitation vehicles and postal trucks
		2019	China VI emission standards for heavy-duty vehicles	Implement China 6a for Gas burning, buses and eventually all heavy-duty vehicles in 2019, 2020 and 2021, respectively. Implement China 6b for gas burning and eventually all heavy-duty vehicles in 2021 and 2023 respectively.
		2020	China VI emission standards for light-duty vehicles	Implement China 6a on 1st July 2020. Implement China 6b on 1st July 2023
Marine emission	HK	2008	Regulations on O_3 depleting substances, NO_x, SO_x, VOC emission, fuel oil quality and shipboard incineration.	
		2015	Ocean going vessel terminated in HK need to switch to <0.5% Sulfur content LPG and other approved fuel	
	HK + Pearl River Delta (PRD)	2019	Air pollution control (Fuel for Vessels) Regulation implement – All marine vessels are required to use compliant fuel within HK and PRD waters	
Power plant	HK	Since 1997	New Coal-fired generating unit by two power companies	
		2008	Fuel Mix Target – Around 50% of the fuel mix for electricity generation is local gas generation.	Two new gas-fired units will be operated in the two power companies in 2023, proportion of gas generation will reach 57%.
		2008-2017	Issue a Technical Memorandum as guideline on emission caps for sulfur dioxide, nitrogen oxides and respirable suspended particulates (PM_{10})	Reduce those pollutants by around 60-80% by 2022 onwards with 2010 as starting year.
		2015	Energy Saving Plan	Reduce energy intensity by 40% by 2025
		2015-2017	State-of-the-art waste-to-energy projects	T·Park (sludge treatment facility) in 2015 (rename in 2016), O·Park (Food waste) in 2014, South-east and West New Territories landfill gases (e.g., CH_4) in 2017.
		2018	Scheme of Control Agreements with two power companies	To encourage development of renewable energy, promotion of energy efficiency, etc.
Power plant (Cont'd)	GD	2014	Nuclear power plants operation with > 9.6 million kW, proportion of non-fossil fuel energy reach > 20% in GD province	By 2017
			Increase electricity transfer from other provinces	By 2017
			Replace coal-power plants with < 100,000 kW capacity with clean energy in PRD	
			Emission control on $PM_{2.5}$ in Thermal Power Plant Air Pollutant Emission Standard, NO_x by low NO_x combustion technologies, SO_2 by desulfurization facility.	
		2019	Regulations on energy consumptions/emitted pollutions including forbidden on building/extending the coal-fired thermal power or captive power station, coal	

			consumption control, promotion on clean energy, restrict high pollution boilers/furnaces, etc.	
Dust	HK	1974	Total emission of dust and grit cannot exceed 0.5%/1.0% of total fuel fired in furnace, oven, or industrial plant with burning rate more/less than 1000 kg per hour	
		1997	Regulations on construction dust including air pollution control system in construction sites, stockpiling of dusty materials, debris handling, excavation or earth moving, etc.	
	China	2008	Technical Specifications for Urban Fugitive Dust Pollution Prevention and Control	
	GD	2017	Promotion of prefabricated building on control of construction dust	By 2020, coverage of prefabricated building in district and prefecture area for > 15% and >10% , respectively
		2019	Regulations on construction dust including air pollution control system in construction sites, debris handling, monitoring via satellite systems, etc.	
Industrial	GD	2009	"Double Transfer" policy – Transfer labor-intensive industries from PRD to less developed regions of the province and subsequent transfer rural labor to the local secondary and tertiary industries or to the PRD region from the primary local industry	
		2012	Industrial Boiler Pollution Control Work Plan – replace with clean energy/ convert into central heating	
		2019	Emission standards of $PM_{2.5}$, SO_2, NOx on (1) steel and cerement & (2) petrochemical industries	
Residential	GD	2014	Forbidden to burn specific fuel including direct burning of biomass in urban districts. Forbidden to burn diesel, kerosene, artificial gas and other gas which beyond emission limit.	

[1] The regulations considered are those under Air Pollution Control Ordinance for Hong Kong and those under Guangdong Action Plan and related regulations in the Pearl River Delta in force during 2007 -2021.

[2] Only regulations/policies on and after 2007 are listed.